Chapter 10
Super-Earths: Atmospheric Accretion, Thermal Evolution and Envelope Loss

Sivan Ginzburg, Niraj K. Inamdar, and Hilke E. Schlichting

Abstract Combined mass and radius observations have recently revealed many short-period planets a few times the size of Earth but with significantly lower densities. A natural explanation for the low density of these super Earths is a voluminous gas atmosphere that engulfs more compact rocky cores. Planets with such substantial gas atmospheres may be a missing link between smaller planets, that did not manage to obtain or keep an atmosphere, and larger planets, that accreted gas too quickly and became gas giants. In this chapter we review recent advancements in the understanding of low-density super-Earth formation and evolution. Specifically, we present a consistent picture of the various stages in the lives of these planets: gas accretion from the protoplanetary disk, possible atmosphere heating and evaporation mechanisms, collisions between planets, and finally, evolution up to the age at which the planets are observed.

10.1 Introduction

The *Kepler* mission discovered a large population of transiting planets a few times the radius of Earth, $R_\oplus$, in orbits of a few to a few dozen days. For a subset of these close-in super Earths we also have a mass measurement from radial velocity or transit timing variation (TTV) observations. Using these combined mass and radius measurements, we find that many of the short-period super Earths have low densities that rule out a purely rocky composition. The low density indicates

S. Ginzburg (✉)
The Hebrew University, Jerusalem 91904, Israel
e-mail: sivan.ginzburg@mail.huji.ac.il

N.K. Inamdar
MIT, Cambridge, MA 02139, USA
e-mail: inamdar@mit.edu

H.E. Schlichting
University of California, Los Angeles, Los Angeles, CA 90095, USA
MIT, Cambridge, MA 02139, USA
e-mail: hilke@epss.ucla.edu

M. Pessah, O. Gressel (eds.), *Formation, Evolution, and Dynamics of Young Solar Systems*, Astrophysics and Space Science Library 445,
DOI 10.1007/978-3-319-60609-5_10

either a water-rich composition or a rocky (or icy) core covered with a voluminous gas atmosphere, which is the only option for many extremely low-density planets (Lopez et al. 2012; Lissauer et al. 2013). Here we adopt the latter interpretation and study the atmospheric accretion onto planetary cores and their evolution. It seems, according to this interpretation, that super Earths with atmospheres of a few % in mass are among the most abundant planets found by *Kepler* (Wolfgang and Lopez 2015).

Rocky cores can gravitationally accrete gas from the gas-rich protoplanetary disk that surrounds young stars for their first few Myr (Mamajek 2009; Williams and Cieza 2011; Alexander et al. 2014). However, explaining the observed low-density super Earths by gas accretion from the surrounding nebula is not trivial. If the gas accretion rate is too fast, a rocky core can acquire an atmosphere comparable to its own mass (Lee et al. 2014). At this stage, the gas accretion rate increases, and the planet quickly evolves into a gas giant (instead of a super Earth) via runaway growth (Bodenheimer and Pollack 1986; Pollack et al. 1996; Piso and Youdin 2014; Piso et al. 2015). If, on the other hand, the accretion is too slow, planets may not obtain substantial atmospheres before the gas disk disperses Moreover, gas atmospheres can be lost due to evaporation (Rogers et al. 2011; Lopez et al. 2012; Owen and Jackson 2012; Lopez and Fortney 2013; Owen and Wu 2013, 2016) or collisions (Inamdar and Schlichting 2015), leaving a bare rocky core behind.

In the following sections we review these various aspects of gas accretion and loss and study the conditions required to form a low-density super Earth. We focus on highlighting the key physical processes that dictate gas accretion and loss and quantify our results in intuitive order of magnitude estimates. Specifically, Sect. 10.2 studies gas accretion from the nebula and Sect. 10.3 discusses mechanisms that can hamper the accretion. Section 10.4 is devoted to the evaporation of atmospheres once the gas nebula disperses. Section 10.5 focuses on the late evolution of low-density super Earths, which is relevant for interpreting the observations of $\sim$Gyr old planets. Section 10.6 discusses atmosphere loss due to giant impacts and the review is summarized in Sect. 10.7.

10.2 Gas Accretion

We assume a rocky core, of mass M_c and radius R_c, embedded inside a gas disk with ambient temperature T_d and density ρ_d. The outer edge, separating the planet's atmosphere from the surrounding nebula, is given by $R_{\rm out} = \min(R_{\rm H}, R_{\rm B})$, with $R_{\rm H}$ and $R_{\rm B}$ denoting the Hill and Bondi radii, respectively. We assume that the atmosphere's mass is $M_{\rm atm} \ll M_c$.

The gas accretion can be divided into two stages, as depicted schematically in Fig. 10.1. Initially, gas adiabatically contracts onto the core in a dynamical timescale. By integrating the adiabatic power-law density profile (Ginzburg et al. 2016), we find that the atmosphere reaches a mass $f \equiv M_{\rm atm}/M_c \propto \rho_d$, which

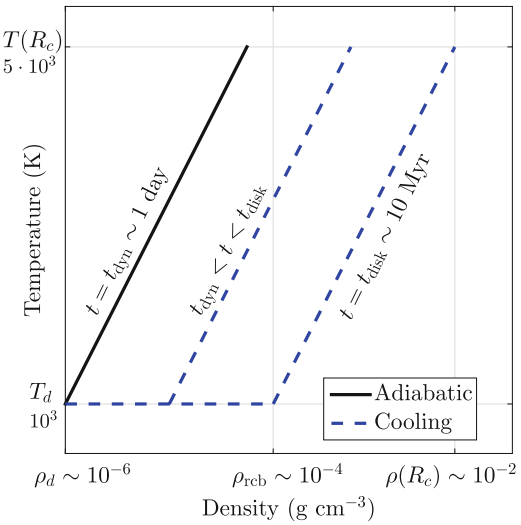

Fig. 10.1 Schematic temperature vs. density profiles (log. scale) of a super-Earth atmosphere during the nebular accretion phase. The initial adiabatic atmosphere (*solid black line*) is isentropic, while at later stages (two successive profiles are plotted) the cooling (and accreting) envelope is characterized by a nearly isothermal radiative outer layer, and a convective interior (*dashed blue lines*). Typical values of the density and temperature are provided. Figure after Ginzburg et al. (2016)

amounts to $f \sim 10^{-3}$, assuming that ρ_d is given by a minimum mass solar nebula (MMSN) model (Hayashi 1981), much lighter than observed envelopes.

Next, the atmosphere cools down and lowers its entropy. During this cooling process, the atmosphere develops an outer radiative, almost isothermal, envelope which is connected to a convective interior at the radiative–convective boundary (RCB), located at $R_{\rm rcb} \lesssim R_{\rm out}$ (Rafikov 2006). $R_{\rm rcb}$ is a good approximation for the planet's actual radius, because beyond it the density drops exponentially with a small scale height. As long as $R_{\rm rcb} \gg R_c$, the temperature profile remains roughly constant, so cooling is equivalent to an increase in density (see Fig. 10.1), and therefore in mass (the radius does not change significantly $R_{\rm rcb} \sim R_{\rm out}$, see Ginzburg et al. 2016). Thus, the planet's accretion rate is determined by the cooling timescale of the atmosphere (Lee et al. 2014; Piso and Youdin 2014). Quantitatively, we find the cooling time by dividing the atmosphere's energy $E_{\rm atm} \propto GM_cM_{\rm atm}$, with G denoting the gravitation constant, by the internal luminosity (calculated by combining the hydrostatic equilibrium and radiative diffusion equations)

$$L = \frac{\gamma - 1}{2} \frac{64\pi}{3} \frac{\sigma T_{\rm rcb}^4 R_{\rm B}}{\kappa \rho_{\rm rcb}}, \tag{10.1}$$

with σ denoting the Stephan-Boltzmann constant, $T_{\rm rcb} \sim T_d$ and $\rho_{\rm rcb}$ denoting the temperature and density at the RCB, and κ the opacity there. γ is the adiabatic index. Notice that the core does not contribute to the energy balance because the temperature on its surface is fixed at a constant $k_{\rm B}T(R_c) \sim GM_c\mu/R_c$ as long as $R_{\rm rcb} \gg R_c$, with $k_{\rm B}$ marking Boltzmann's constant and μ the molecular mass. Intuitively, the luminosity can be understood as $L \sim \sigma T_{\rm rcb}^4 R_{\rm rcb}^2/\tau$, with τ marking the optical depth at the RCB. The opacity increases mildly with the density (Freedman

et al. 2008, 2014), implying, due to Eq. (10.1), that $L \propto \rho_{\rm rcb}^{-1} \propto M_{\rm atm}^{-1}$ (only the convective part of the atmosphere contributes significantly to the mass). Finally, we obtain the growth of the atmosphere with time $t = E_{\rm atm}/L \propto M_{\rm atm}^2(t)$ (Piso and Youdin 2014). Specifically, Ginzburg et al. (2016) find that by the time the disk disperses $t = t_{\rm disk}$, the atmosphere's mass fraction is given by

$$f \approx 0.02 \left(\frac{M_c}{M_\oplus}\right)^{0.8} \left(\frac{T_d}{10^3\ {\rm K}}\right)^{-0.25} \left(\frac{t_{\rm disk}}{1\ {\rm Myr}}\right)^{0.5}, \tag{10.2}$$

with $M_\oplus$ marking Earth's mass (see Lee and Chiang 2015, for a similar result).

We notice that while the mass of the initial adiabatic atmosphere is proportional to the nebula's density, Eq. (10.2) does not depend on ρ_d. More precisely, the dependence on ρ_d is logarithmic, and is therefore omitted (see Ginzburg et al. 2016). Intuitively, the radiative envelope decouples the density of the atmosphere $\propto \rho_{\rm rcb}$ from the outer boundary condition ρ_d (see Fig. 10.1). Thus, the bottleneck that typically determines the accretion rate is not the amount of available gas, but rather the rate at which this gas can radiate away its gravitational energy and settle onto the core. The logarithmic dependence on ρ_d implies that significant atmospheres can be accreted even in highly depleted disks (Inamdar and Schlichting 2015; Lee and Chiang 2016). Such depleted (and short lived, so $f \propto t_{\rm disk}^{1/2}$ is smaller) disks are relevant if atmosphere accretion is delayed until the assembly of the rocky core by collisions is over (see Sect. 10.6).

10.3 Atmosphere Heating

In Sect. 10.2 we demonstrated that atmosphere accretion is equivalent to cooling. Therefore, mechanisms that heat the atmosphere can hamper gas accretion. Such mechanisms have the potential to explain why super Earths did not continue to grow into gas giants, if accretion is somewhat more efficient than in Eq. (10.2), as suggested by Lee et al. (2014). In this section we focus on two examples: heating by planetesimals and by tides.

10.3.1 Heating by Planetesimals

The formation of the rocky cores of super-Earths and of gas giants can be divided into two phases (see, e.g., Goldreich et al. 2004). In the first phase, the cores grow by gravitationally attracting small building blocks (planetesimals) into their Hill sphere. The final mass in this phase is referred to as the "isolation mass". In the next phase, these isolation masses collide with each other due to orbital instability. This phase is referred to as the "giant impacts" phase.

The loss of gravitational energy of the impacting planetesimals dissipates heat inside the growing planet. The timescale for the core growth of giant planets in the outer disk is comparable to the gas disk lifetime, a few Myr (Pollack et al. 1996). Therefore, the accretion of solids and gas is simultaneous, and heating by planetesimals plays a crucial role in the cooling (equivalent to growth) of the gas atmosphere (Rafikov 2006, 2011). In the inner disk, however, the solid accretion time is shorter, implying that the core formation may be decoupled from the atmosphere growth (Lee et al. 2014). For this reason, many studies ignore planetesimal heating in the context of the close-in *Kepler* super Earths. However, a steady stream of new planetesimals may be supplied from larger semi-major axes as the planetesimal orbits decay due to their interaction with the gas disk. Even if the bulk of the planetesimals is consumed at an early stage (on a timescale much shorter than $t_{\rm disk}$), residual impacting debris can still interfere with the growth of the atmosphere.

How does the accretion of a solid mass ΔM_c during the disk's lifetime $t_{\rm disk}$ affect the gas accretion? We assume that the planetesimals impact at a constant rate and deposit their energy at the surface of the rocky core. In this case, the accretion luminosity is given by $L_{\rm acc} = GM_c\Delta M_c/(R_c t_{\rm disk})$. The internal luminosity at the end of accretion (when $t = t_{\rm disk}$), on the other hand, is given by $L = GM_c M_{\rm atm,0}/(R_c t_{\rm disk})$, assuming that the atmosphere's energy and mass are concentrated near R_c. This is relevant for the low values of γ, found by Lee et al. (2014) and Piso et al. (2015), due to hydrogen dissociation. $M_{\rm atm,0}$ marks the final atmosphere mass, if planetesimal impacts are ignored, which is calculated in Sect. 10.2. Since, according to Eq. (10.1), $L \propto M_{\rm atm}^{-1}(t)$, the internal luminosity reaches its minimum at the end of accretion ($t = t_{\rm disk}$). Therefore, if $\Delta M_c < M_{\rm atm,0}$ then $L_{\rm acc} < L$ during the accretion phase, and the heat generated by planetesimal impacts is evicted from the planet without affecting gas accretion.

For $\Delta M_c > M_{\rm atm,0}$, the internal luminosity L drops below the planetesimal-generated heat $L_{\rm acc}$ before the atmosphere reaches its final mass. Quantitatively, using $L \propto M_{\rm atm}^{-1}(t)$, the luminosities are equal when $M_{\rm atm}(t) = M_{\rm atm,0}^2/\Delta M_c$. At this stage gas accretion stops and the final atmosphere mass is therefore given by

$$\frac{M_{\rm atm}}{M_{\rm atm,0}} = \begin{cases} M_{\rm atm,0}/\Delta M_c & \Delta M_c > M_{\rm atm,0} \\ 1 & \Delta M_c < M_{\rm atm,0} \end{cases}. \tag{10.3}$$

Equation (10.3) shows that a mass in planetesimals comparable to the final atmospheric mass, $M_{\rm atm,0}$, can stop the gas accretion. This is interesting since the mass-radius relation for many close-in exoplanets suggests that they are enshrouded in gaseous envelopes containing a few percent of the planet's mass such that the accretion of planetesimals containing a few percent of an Earth's mass could lead to an early termination of the gas accretion. This is particularly interesting since the Earth is believed to have accreted about 1% of its total mass after the Moon-forming impact, suggesting that a planetesimal population containing a few % of an Earth mass did survive over time scales of 10^7–10^8 years in the inner solar system (Walker 2009; Schlichting et al. 2012). Equation (10.3), however, also demonstrates

that heating by planetesimals cannot stop super Earths from evolving into gas giants by runaway gas accretion (see Sect. 10.1). The reason is that runaway accretion initiates when $M_{\rm atm} \sim M_c$ and the accreted gas significantly increases the planet's mass (and therefore its ability to attract more gas). In order to intervene with the accretion of such heavy atmospheres, Eq. (10.3) requires $\Delta M_c \sim M_c$, leading to faster gas accretion and runaway growth. Lee and Chiang (2015) reach the same conclusion by considering the non-linear relation between the atmosphere's mass and the planet's luminosity, which is more accurate for heavy, self-gravitating, atmospheres $M_{\rm atm} \sim M_c$.

We note that, in addition to their accretion heat, planetesimal impacts may also affect atmosphere growth by enhancing the atmosphere's heavy-element abundance, and therefore the opacity κ. We do not discuss this effect here.

In Sect. 10.6 we discuss the effects of the second phase of the core's assembly—giant impacts between the isolation masses.

10.3.2 Tidal Heating

Tidal heating has been proposed as a mechanism to inhibit the cooling of close-in gas giants (hot Jupiters), thus halting their contraction and explaining their puzzlingly large radii (Bodenheimer et al. 2001, 2003; Gu et al. 2003; Winn and Holman 2005; Jackson et al. 2008; Liu et al. 2008; Ibgui and Burrows 2009; Miller et al. 2009; Ibgui et al. 2010, 2011; Leconte et al. 2010). Can the same mechanism interfere with the cooling (and thereby accretion) of super-Earth atmospheres?

Ginzburg and Sari (2017) find the heat dissipation in the atmosphere due to circularizing tides

$$L_{\rm circ} = \frac{63\pi}{2} f \frac{e^2}{QP} \frac{GM_\odot^2}{R_{\rm rcb}} \left(\frac{R_{\rm rcb}}{a}\right)^6 \propto M_{\rm atm} R_{\rm rcb}^5, \tag{10.4}$$

with e denoting the orbital eccentricity, $Q \sim 10^5$ the tidal dissipation parameter of the atmosphere, $M_\odot$ the stellar mass, a the semi-major axis, and P the orbital period. During accretion, $R_{\rm rcb} \approx 0.5 R_{\rm out} = 0.5 \min(R_{\rm H}, R_{\rm B})$ (Ginzburg et al. 2016) is larger than the radius of Jupiter, leading to strong tidal heating, due to Eq. (10.4). The tidal power increases as $L_{\rm circ} \propto M_{\rm atm}(t)$, while the cooling luminosity decreases as $L \propto M_{\rm atm}^{-1}(t)$, according to Eq. (10.1). Therefore, atmosphere accretion will stop when $L = L_{\rm circ}$ and the tidal heat can no longer be evicted from the planet. If the tidal heating is strong enough (i.e., the planet is close to the star), then this condition is reached when $t < t_{\rm disk}$ and the atmosphere does not reach its full mass potential $M_{\rm atm,0}$, similar to Sect. 10.3.1. Quantitatively, from Ginzburg and Sari (2017):

$$\frac{M_{\rm atm}}{M_{\rm atm,0}} = \begin{cases} (P/P_{\rm crit})^{5/6} & P < P_{\rm crit} \\ 1 & P > P_{\rm crit} \end{cases}, \tag{10.5}$$

with $P_{\rm crit}$ marking the critical period, beyond which tides do not affect atmosphere accretion, given by

$$e \sim \left(Q\frac{P_{\rm crit}}{t_{\rm disk}}\right)^{1/2}\left(\frac{P_{\rm crit}}{t_{\rm dyn}}\right)^{1/3} \sim 0.2\left(\frac{P_{\rm crit}}{10\ {\rm day}}\right)^{5/6}, \tag{10.6}$$

for $t_{\rm disk} = 3$ Myr and with the core's dynamical time given by $t_{\rm dyn} \equiv (G\rho_c)^{-1/2} \approx 0.5$ h ($\rho_c \approx 5\,{\rm g\,cm^{-3}}$ is the rocky core's mean density). By combining Eqs. (10.2), (10.5), and (10.6) we obtain (see Ginzburg and Sari 2017, for details) the maximum gas mass fraction a rocky core may accrete when tides are taken into account, so that $f = \min(f_0 \equiv M_{\rm atm,0}/M_c, f_{\rm max})$ with

$$f_{\rm max} \approx \frac{2\%}{e}\left(\frac{M_c}{5M_\oplus}\right)^{0.8}\left(\frac{P}{10\ {\rm day}}\right)^{19/21}. \tag{10.7}$$

Equation (10.7) demonstrates that large eccentricities $e \gtrsim 0.2$ are necessary for tides to play a role in shaping super-Earth atmospheres. Due to the gas damping, such eccentricities are usually considered unlikely during the nebular phase. However, some studies suggest that planet–disk interactions may, under some circumstances, excite, rather than damp, the eccentricity (Goldreich and Sari 2003; Duffell and Chiang 2015; Teyssandier and Ogilvie 2016). Ginzburg and Sari (2017) find circularization timescales $t_{\rm circ} \sim 10^8$ yr $\ll$ Gyr (after the gas disk disperses). These relatively short timescales allow planets to cool, contract, and reach their observed radii after the tidal heating has ceased (see Sect. 10.5). In addition, the short timescales are consistent with the small observed eccentricities in Gyr-old systems.

Tidal heating has the potential to explain why super-Earths did not reach $f \sim 1$ and grow into Jupiters via runaway accretion. In addition, the dependence of $f_{\rm max}$ on the orbital period, as demonstrated in Eq. (10.7), might explain the scarcity of low-density super Earths in close proximity to the star (e.g. Youdin 2011). Nevertheless, in the following sections we ignore tides and focus on an alternative mechanism that may sculpt the observed super-Earth population—atmosphere evaporation.

10.4 Evaporation

After the gas disk disperses atmospheres can no longer grow in mass. At this stage, super-Earth evolution is governed by two processes: evaporation and cooling, which is now equivalent to contraction, rather than accretion (since the density increases with a constant $M_{\rm atm}$, see Ginzburg et al. 2016, for details).

Atmosphere evaporation can result from various mechanisms, with photoevaporation by high-energy stellar radiation commonly considered (Rogers et al. 2011; Lopez et al. 2012; Owen and Jackson 2012; Lopez and Fortney 2013; Owen and

Wu 2013; Lundkvist et al. 2016). The basic picture is that ionizing photons release energetic electrons which in turn heat the gas to high temperatures above the escape velocity. If the cooling of the gas is slow enough, the high-temperature gas escapes the planet's potential well. The widely used energy-limited model for photoevaporation linearly relates the gravitational energy of the escaping mass to the incident ionizing flux, so that the evaporation timescale of the atmosphere is given by $t_{\rm evap} \propto M_{\rm atm}/(\epsilon T_{\rm eq}^4)$. $T_{\rm eq}$ marks the equilibrium temperature on the planet's surface and ϵ accounts for both the evaporation efficiency and the fraction of the ionizing radiation out of the total bolometric flux. ϵ is considered to be approximately constant for $t_{\rm UV} \sim 100$ Myr, while the star is UV active, and then it decreases with time as $\epsilon \propto t^{-1.25}$ (Jackson et al. 2012; Lopez et al. 2012; Owen and Jackson 2012, and references therein). For $t > t_{\rm UV}$ the ratio of evaporation timescale to age increases as $t_{\rm evap}/t \propto t^{0.25}$. Therefore, if an atmosphere survived until $t_{\rm UV}$, it will keep most of its mass in later times.

In addition to evaporation by external irradiation, mass from the loosely bound outer layers of the atmosphere can also be lost spontaneously, due to heat from the contracting inner layers of the atmosphere or from the underlying rocky core, combined with loss of pressure support from the vanishing gas-disk (Ikoma and Hori 2012; Owen and Wu 2016; Ginzburg et al. 2016). In fact, since the cooling luminosity of the planet is the energy source unbinding the outer atmosphere, the ratio between the cooling and evaporation timescales is simply the ratio between the atmosphere's energy (concentrated in its inner layers) and the binding energy of the outer layers

$$\frac{t_{\rm evap}}{t_{\rm disk}} = \frac{t_{\rm evap}}{t_{\rm cool}} = \frac{E_{\rm evap}}{E_{\rm atm}} = \left(\frac{R_{\rm rcb}}{R_c}\right)^{-(3-2\gamma)/(\gamma-1)}, \tag{10.8}$$

where the last equality is derived for atmospheres that have their energy concentrated in the inner layers, while mass in the outside (as for the diatomic $\gamma = 7/5$. See Ginzburg et al. 2016, for derivation and other cases). Equation (10.8) shows that evaporation dominates super-Earth evolution (after disk dispersal) as long as $R_{\rm rcb} \gg R_c$. Therefore, super Earths spontaneously shed their outer layers (dozens of percents in mass) and shrink to a radius comparable to R_c. Moreover, since $t_{\rm cool} = t_{\rm disk}$ by definition when the disk disperses and it can be shown that $t_{\rm cool}$ remains constant during the evaporation, the mass shedding occurs on a timescale comparable to $t_{\rm disk}$.

10.4.1 Thin Atmosphere

After a time $\sim t_{\rm disk}$ (a few Myr) atmospheres shrink from their initial size $\sim R_{\rm out}$ to a radius comparable to the size of the rocky core R_c, as explained above. To study this regime, we redefine $R_{\rm rcb} \equiv R - R_c$, where R is the radius of the RCB (essentially, the planet's radius). This definition coincides with the previous one for the thick

atmosphere regime ($R_{\rm rcb} \gg R_c$). As in the thick regime, the thin regime is also characterized by a competition between cooling (i.e. contraction) and evaporation. While photoevaporation does not change conceptually in this phase, spontaneous evaporation may differ dramatically in the thin regime.

During the thick phase, the temperature at the base of the atmosphere, and therefore the temperature on the surface of the adjacent core remains constant $k_{\rm B}T(R_c) \sim GM_c\mu/R_c$. Therefore, assuming the core is convective (a plausible assumption for high temperatures for which the core is molten), it does not cool and its temperature profile remains constant. In the thin regime, however, an adiabatic atmosphere dictates the following temperature at its base:

$$k_{\rm B}T(R_c) = k_{\rm B}T_d + \frac{GM_c\mu}{R_c}\frac{R_{\rm rcb}}{R_c} \approx \frac{GM_c\mu}{R_c}\frac{R_{\rm rcb}}{R_c}, \tag{10.9}$$

where the last approximation assumes that the atmosphere is not ultra-thin $R_{\rm rcb}/R_c > R_c/R_{\rm B}$ (see Ginzburg et al. 2016). Equation (10.9) shows that once $R_{\rm rcb} < R_c$, the temperature on the surface of the rocky core becomes dependent on the thickness of the atmosphere $R_{\rm rcb}$. Consequently, as the atmosphere cools (and contracts), $T(R_c) \propto R_{\rm rcb}$ decreases, so the rocky core cools as well. Thus, while for $R_{\rm rcb} > R_c$ the rocky core does not play a role in the planet's cooling, for $R_{\rm rcb} < R_c$ we have to take into account its heat capacity. Quantitatively, the available energy for cooling in the thin regime is

$$E = gR_{\rm rcb}\left(\frac{\gamma}{2\gamma-1}M_{\rm atm} + \frac{1}{\gamma}\frac{\gamma-1}{\gamma_c-1}\frac{\mu}{\mu_c}M_c\right), \tag{10.10}$$

with $g \equiv GM_c/R_c^2$ denoting the surface gravity and μ_c and γ_c marking the rocky core's molecular weight and adiabatic index, respectively. The first term in Eq. (10.10) represents the (gravitational and thermal) energy of the gaseous atmosphere and the second term accounts for the heat capacity of the rocky core (which is approximately incompressible).

In summary, during the thin phase we distinguish, following Eq. (10.10), between heavy atmospheres ($f \gtrsim \mu/\mu_c$), that regulate their own cooling, and light atmospheres ($f \lesssim \mu/\mu_c$), that are dominated by the heat capacity of the underlying rocky core. Assuming that the atmosphere is composed of hydrogen and helium and the core has an Earth-like composition, the above distinction is at a mass fraction of a few percent. The binding energy of the thin atmosphere is $E_{\rm evap} = GM_cM_{\rm atm}/R_c = gM_{\rm atm}R_c$. Therefore, heavy atmospheres cool and contract without spontaneous evaporation (since $R_{\rm rcb} < R_c$ and $E < E_{\rm evap}$). Light atmospheres, on the other hand, are lost completely because when they enter the thin regime $R_{\rm rcb} = R_c$ and $E > E_{\rm evap}$. Consequently, the atmosphere cannot cool and contract, and therefore $R_{\rm rcb} \propto E$ remains constant while $M_{\rm atm}$ evaporates (see Ginzburg et al. 2016, for details). One consideration that can save light atmospheres from complete

loss is the loss timescale which can exceed the age of the system, in which case light atmospheres can survive to the present day not because there is insufficient energy to complete the loss but simply because their loss timescales exceed several Gyrs.

10.4.2 The Goldilocks Region

As explained in Sect. 10.1, acquiring and preserving atmospheres of a few percent from the protoplanetary disk is not trivial. If a rocky core is too massive or too cold (i.e. far away from the star), it will acquire an atmosphere which is too massive, according to Eq. (10.2), reaching $f \sim 1$ and then evolving via runaway accretion into a gas giant instead of a super-Earth. On the other hand, if the rocky core is too light or too close to the star, it will obtain a light atmosphere which is susceptible to evaporation, since $t_{\rm evap} \propto M_{\rm atm}/(\epsilon T_{\rm eq}^4)$ for photoevaporation, as explained above (spontaneous evaporation acts qualitatively similar).

In Fig. 10.2 we present the Goldilocks region in which rocky cores can accrete H/He envelopes at their current location, becoming low-density super Earths. Planets above the "Jupiter" line explode into Jupiters, while planets below the "UV" line lose their atmospheres due to UV photoevaporation. In the shaded area

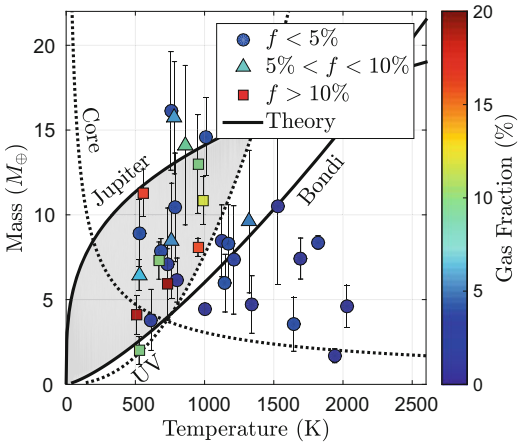

Fig. 10.2 Observed super-Earth population from Weiss and Marcy (2014). The planets are grouped according to their gas mass fraction f, estimated by Eq. (10.12), with low-density planets marked by *triangles* ($5\% < f < 10\%$) or *squares* ($f > 10\%$). The planet markers are also colour-coded according to f. The *top solid line* ("Jupiter") is according to Eq. (10.2) with $t_{\rm disk} = 10$ Myr and $f = 0.5$, while the *bottom dashed line* ("UV") represents the condition to survive photoevaporation $t_{\rm evap} \propto M_{\rm atm}/(\epsilon T_{\rm eq}^4) > t_{\rm UV}$. The other lines ("Core" and "Bondi") are relevant for spontaneous evaporation (see Ginzburg et al. 2016, for details). Inside the shaded area, planets manage to accrete and maintain gas envelopes without exploding into gas giants due to runaway accretion. Figure after Ginzburg et al. (2016)

between these lines we expect to find low-density super Earths. As seen in the figure, the observed low-density super-Earth population is indeed concentrated in the Goldilocks region, with mainly bare rocky cores outside it.

Migration can extend the Goldilocks region by separating the gas accretion from the UV evaporation, allowing planets to grow their atmospheres in more favourable conditions (see Ginzburg et al. 2016, for details).

10.5 Late Evolution

In Sect. 10.2 we discussed gas accretion from the protoplanetary disk, which vanishes after $t_{\rm disk} \sim 3$ Myr. In Sect. 10.4 we studied the evolution following disk dispersal. This consists of spontaneous evaporation for $\sim t_{\rm disk}$, in which the atmosphere shrinks to a thickness $R_{\rm rcb} \sim R_c$, followed by photoevaporation for $t_{\rm UV} \sim 100$ Myr, which evaporates the atmospheres of light or hot (i.e. close to the star) rocky cores. However, the planets that we observe are $\sim$Gyrs old. In this section we focus on the late evolution of low-density super Earths, after photoevaporation has ceased to play a role.

At an age $t > t_{\rm UV}$, heavy envelopes ($f \gtrsim \mu/\mu_c$, see Sect. 10.4.1) cool and contract with a constant mass $M_{\rm atm}$. Quantitatively, the atmosphere's mean density is determined by the adiabatic relation $\rho/\rho_{\rm rcb} \sim (T(R_c)/T_d)^{1/(\gamma-1)} \propto R_{\rm rcb}^{1/(\gamma-1)}$, with the last relation from Eq. (10.9). Since the atmosphere's mass is given by $M_{\rm atm} \sim \rho R_c^2 R_{\rm rcb}$, we find that $\rho_{\rm rcb} \propto R_{\rm rcb}^{-\gamma/(\gamma-1)}$. We combine this result with Eqs. (10.1) and (10.10) and derive the contraction of the atmosphere with time $t = E/L \propto R_{\rm rcb}^{-1/(\gamma-1)}$.

For the diatomic $\gamma = 7/5$, gas envelopes contract as $R_{\rm rcb} \propto t^{-2/5}$. However, gas envelopes do not compress indefinitely, and at some stage they reach the $T_{\rm eq}$ temperature floor, or the maximal gas density ceiling $\rho_{\rm max}$, becoming liquid. Ginzburg et al. (2016) use the scaling relation above to show that super-Earth atmospheres reach $\rho_{\rm max}$ in a few Gyrs. Numerical evolution models (e.g. D'Angelo and Bodenheimer 2016) confirm that gas atmospheres stop contracting after $\sim$10 Gyr, somewhat longer than the approximate estimate in Ginzburg et al. (2016). For simplicity, we assume here that atmospheres of observed planets are close to $\rho_{\rm max}$, approximately consistent with the analytical and numerical estimates above. We evaluate this density using the equation of state of Nettelmann et al. (2008) as

$$\rho_{\rm max} \approx 0.5\,{\rm g\,cm^{-3}} \left(\frac{p}{\rm Mbar}\right)^{0.4}, \tag{10.11}$$

with $p \approx M_{\rm atm} g/(4\pi R^2)$ denoting the typical atmospheric pressure.

With the above estimate for the atmosphere's density, we can infer an observed planet's atmosphere mass fraction $f \equiv M_{\rm atm}/M_c$ from its mass $M \approx M_c$ and radius R by

$$f = \frac{\rho_{\rm max}}{\rho_c}\left[\left(\frac{R}{R_c}\right)^3 - 1\right], \tag{10.12}$$

with the rocky core's density and radius given by $\rho_c \propto R_c \propto M_c^{1/4}$, taking into account the mild gravitational compression (e.g. Valencia et al. 2006). Our estimate for the observed f is displayed in Fig. 10.3. This crude estimate is in agreement (approximately) with more elaborate numerical time-dependent estimates, e.g., Lopez et al. (2012).

It is important to mention that heating mechanisms can change our interpretation of the density, and therefore of f. Because cooling is equivalent to contraction in these late evolutionary stages, heating mechanisms can slow down or stop the contraction, in a similar manner to their effect on accretion in earlier stages (see Sect. 10.3). While tidal heating cannot stop contraction for long ($t_{\rm circ} \ll$ Gyr, see Sect. 10.3.2), Ohmic heating due to interaction of atmospheric winds with the planet's magnetic field might play an important role (see Valencia and Pu 2015). Heating mechanisms that delay contraction imply that the values of f given in Fig. 10.3 and in Lopez et al. (2012) might be overestimated, due to an overestimate of the density at a given age.

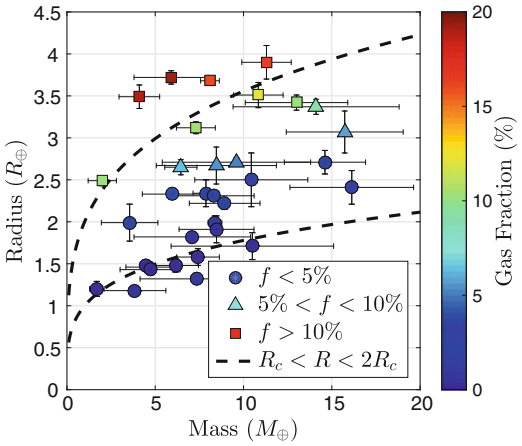

Fig. 10.3 Observed super-Earth population from Weiss and Marcy (2014). The planets are grouped according to their gas mass fraction f, estimated by Eq. (10.12), with low-density planets marked by *triangles* ($5\% < f < 10\%$) or *squares* ($f > 10\%$). The planet markers are also colour-coded according to f. The *two dashed black lines* mark the radius of the rocky core $R_c(M_c)$ and $2R_c(M_c)$. Planets with substantial atmospheres are expected to be found roughly between the two lines. Figure after Ginzburg et al. (2016)

10.6 Diversity of the Super-Earth Population and Giant Impacts

In the previous sections we showed that with simple physical arguments we can define a relatively narrow mass/temperature range in which planets are massive and cold enough to acquire and retain a significant atmosphere, while not too massive and cold to undergo runaway gas accretion and turn into Jupiters. Figure 10.2 shows that observed low-density super-Earths indeed reside in the predicted range of our model. However, the diversity among these super-Earths in terms of the total amount of gas they accreted is not well explained by our model, since, as we show in Eq. (10.2), the amount of accreted gas is primarily a function of core mass, temperature and disk lifetime. In addition, many observed exoplanetary systems that are in tightly packed orbital configurations also show significant diversity in their gas-mass fractions and bulk densities (see Fig. 10.4). Both of these observations are challenging to explain by gas accretion and subsequent sculpting by photo-evaporation alone. We suggest that the large observed range in exoplanet bulk densities maybe due to one or two giant impacts that occurred late in their evolution once the gas disk dissipated. We show below that giant impacts can modify the bulk composition of a super-Earth by factors of a few and in some cases lead to complete atmospheric loss (Inamdar and Schlichting 2016; Liu et al. 2015). Such late giant impacts are likely to be common because super-Earths must have formed in the presence of the gas disk and their dynamical interaction with the disk is expected to have resulted in migration and efficient eccentricity damping leading to densely packed planetary systems. As the gas disk dissipated mutual excitations lead to eccentricity growth culminating in one or two giant impacts ultimately resulting in planetary systems with long-term stability (Cossou et al. 2014).

10.6.1 Giant Impacts and Atmospheric Mass Loss

We use one-dimensional hydrodynamic simulations to calculate the envelope mass loss resulting from a giant impact. As the giant impact occurs it launches a strong shock that transverses the entire planet and that results in a global ground motion that in turn launches a shock into the atmosphere (see Fig. 10.5). We only model the adiabatic part of the atmosphere since the isothermal outer layer contains negligible mass. The propagation of the shock in the atmosphere is tracked by solving the hydrodynamic equations with a finite-difference Lagrangian scheme. If a fluid parcel is accelerated to velocities above its initial escape velocity from the planet, it is considered lost. The global mass loss is determined by integrating the local mass loss over the entire surface of the planet accounting for the global distribution of the different ground velocities (see Inamdar and Schlichting 2016, for details).

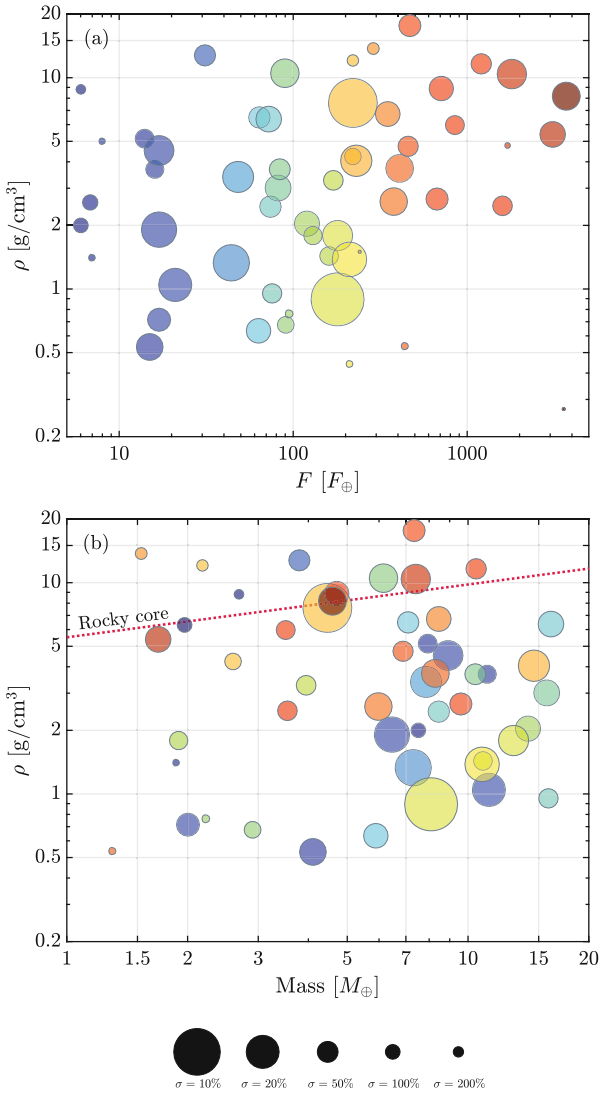

Fig. 10.4 Densities of exoplanets with $R < 4R_\oplus$. The surface area of each data point is inversely proportional to the 1σ error of the density estimate, such that the most secure density measurements correspond to the largest points. The normalization of the error bars is shown at the *bottom*. The colours of the points represent the amount of flux received from the host star. (**Panel a**) shows mean density as a function of flux, F, in units of the Earth flux, $F_\oplus$. (**Panel b**) displays exoplanet densities as a function of planet mass in units of Earth masses, $M_\oplus$. Most data are taken from Weiss and Marcy (2014) and the references therein. Additional data taken from Jontof-Hutter et al. (2015) and Barros et al. (2015). For reference, a mean density curve assuming a purely rocky planet (Seager et al. 2007) is shown with a *dotted red line*. Figure after Inamdar and Schlichting (2016)

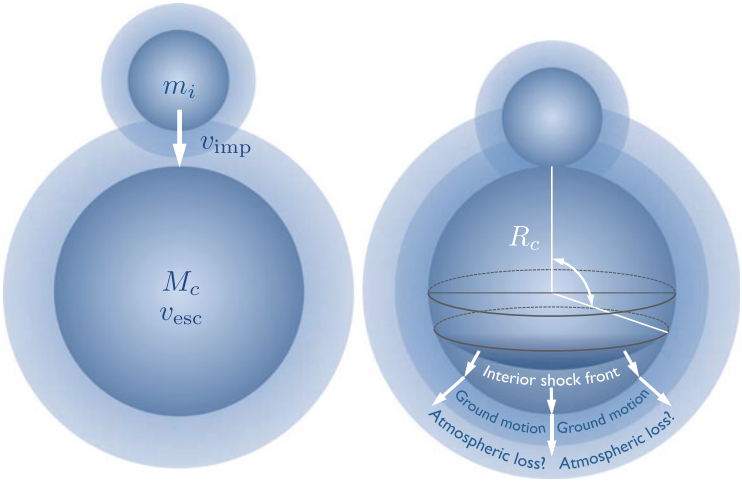

Fig. 10.5 The geometry of a giant impact. On the *left*, an impactor of mass m_i and impact velocity $v_{\rm imp} \sim \sqrt{2} v_{\rm esc}$ approaches a target of mass M_c and escape velocity $v_{\rm esc}$. After the collision, a shock is generated through the target core. The shock—which propagates so as to conserve the linear momentum of the impactor—results in ground motion on the target body. This ground motion launches a shock into the overlying gas envelope, leading to hydrodynamic mass loss. For further details, see Inamdar and Schlichting (2015)

Figure 10.6 displays the global atmospheric loss as a function of the momentum of the impact. The results are displayed for atmospheric mass fraction of $f = 1\%$ and $f = 5\%$ spanning typical values for the mass fraction of super-Earth envelopes. By conservation of energy, the speed at which the two bodies collide with one another, $v_{\rm imp}$, is given by $v_{\rm imp}^2 = v_{\rm esc}^2 + v_\infty^2$, where $v_{\rm esc} = \sqrt{2G(M_c + m_i)/(R_c + r_i)}$ is the mutual escape velocity of the two bodies and v_∞ the (relative) velocity dispersion of the two bodies. Here, M_c and m_i are the mass of the target and impactor, respectively and R_c and r_i are their corresponding radii. The largest protoplanets/planets will gravitationally stir the other bodies around them, exciting the velocity dispersion to roughly $v_{\rm esc}$, so that $v_{\rm imp} \sim \sqrt{2} v_{\rm esc}$. Such that for equal mass impactors, the normalized impactor momentum is $\sim$0.7 implying that roughly half of the total envelope will be lost. This in turn will modify the bulk density of super-Earths by a factor of a few as shown in Inamdar and Schlichting (2016).

This atmospheric mass loss calculated in Fig. 10.6 is likely an underestimate of the total envelope loss because even the part of the envelope that was not immediately lost in the impact is susceptible to subsequent loss by photo-evaporation and Parker winds (Liu et al. 2015) because of its large inflated radius after the collision.

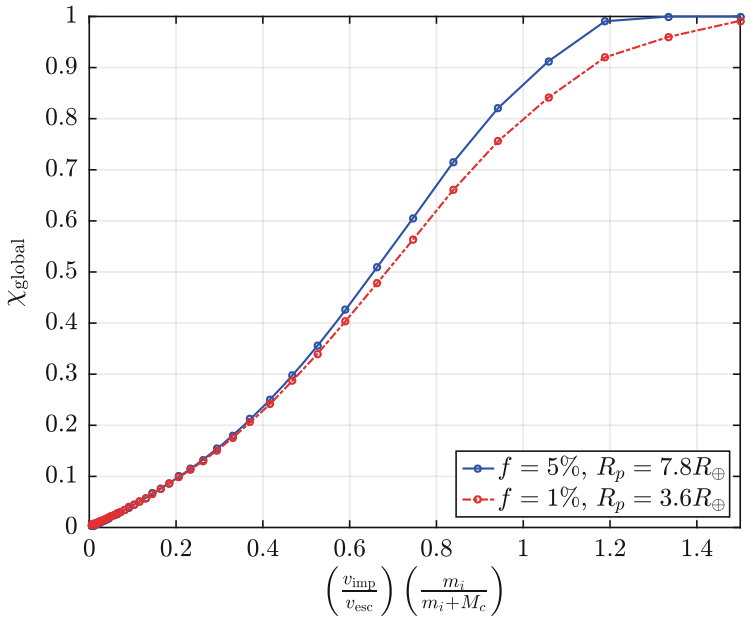

Fig. 10.6 Mass loss curve for late stage giant impacts. On the *vertical axis*, we show the envelope mass loss fraction due to a giant impact. On the *horizontal axis*, we show impactor linear momentum normalized to $M_c v_{\rm esc}$. After the dissipation of the gas disk, the radial extent and structure of the envelope depends on the planet's cooling history. Here we assume $4M_\oplus$ core and envelope mass fractions of $f = 1\%$ (*red line*) and $f = 5\%$ (*blue line*). The total planet radii correspond to results from thermal evolution models after 50 Myr of cooling at 0.1 AU. A typical late stage merger between equal mass impactors (such that the normalized impactor momentum on the horizontal axis is $\sqrt{2}/2 \approx 0.7$) results in roughly half of the envelope mass being stripped away. Figure after Inamdar and Schlichting (2016)

10.7 Summary

In this chapter we studied the formation and evolution of voluminous gas atmospheres of short-period super Earths. Such gas envelopes, which constitute a few percent of the planet's mass, are a possible explanation to the low densities of many observed planets.

We showed that with simple physical arguments we can define a relatively narrow mass/temperature range in which planets are massive and cold enough to acquire and retain a significant atmosphere, while not too massive and cold to undergo runaway gas accretion and turn into Jupiters. Figure 10.2 shows that observed low-density super-Earths indeed reside in the predicted range of our model. However, the diversity among these super-Earths in terms of the total amount of gas they accreted is not well explained by gas accretion and subsequent sculpting by photo-evaporation alone.

We show that giant impacts can modify the bulk composition of a super-Earth by factors of a few and in some cases lead to complete atmospheric loss (Inamdar and Schlichting 2016; Liu et al. 2015) and suggest that giant impacts maybe responsible for the large observed range in exoplanet bulk densities, especially in tightly packed multiple planet systems.

In summary, explaining the low densities of close-in super Earths by gas accretion from the surrounding nebula has been the focus of intensive study for the last few years. While the different studies converge to a consistent understanding of the accretion itself, the importance of other mechanisms, such as heating (during or after gas accretion), migration (see D'Angelo and Bodenheimer 2016), and collisions are subject of active research.

Acknowledgements We thank Re'em Sari for discussions.

References

Alexander, R., Pascucci, I., Andrews, S., Armitage, P., Cieza, L.: The dispersal of protoplanetary disks. In: Protostars and Planets VI, pp. 475–496. University of Arizona Press, Tuscon (2014). 1311.1819

Barros, S.C.C., Almenara, J.M., Demangeon, O., Tsantaki, M., Santerne, A., Armstrong, D.J., Barrado, D., Brown, D., Deleuil, M., Lillo-Box, J., Osborn, H., Pollacco, D., Abe, L., Andre, P., Bendjoya, P., Boisse, I., Bonomo, A.S., Bouchy, F., Bruno, G., Cerda, J.R., Courcol, B., Díaz, R.F., Hébrard, G., Kirk, J., Lachurié, J.C., Lam, K.W.F., Martinez, P., McCormac, J., Moutou, C., Rajpurohit, A., Rivet, J.P., Spake, J., Suarez, O., Toublanc, D., Walker, S.R.: Photodynamical mass determination of the multiplanetary system K2-19. Mon. Not. R. Astron. Soc. **454**, 4267–4276 (2015). 1510.01047

Bodenheimer, P., Pollack, J.B.: Calculations of the accretion and evolution of giant planets The effects of solid cores. Icarus **67**, 391–408 (1986)

Bodenheimer, P., Lin, D.N.C., Mardling, R.A.: On the tidal inflation of short-period extrasolar planets. Astrophys. J. **548**, 466–472 (2001)

Bodenheimer, P., Laughlin, G., Lin, D.N.C.: On the radii of extrasolar giant planets. Astrophys. J. **592**, 555–563 (2003). astro-ph/0303541

Cossou, C., Raymond, S.N., Hersant, F., Pierens, A.: Hot super-Earths and giant planet cores from different migration histories. Astron. Astrophys. **569**, A56 (2014). 1407.6011

D'Angelo, G., Bodenheimer, P.: In Situ and Ex Situ formation models of Kepler 11 planets. Astrophys. J. **828**, 33 (2016). 1606.08088

Duffell, P.C., Chiang, E.: Eccentric Jupiters via disk-planet interactions. Astrophys. J. **812**, 94 (2015). 1507.08667

Freedman, R.S., Marley, M.S., Lodders, K.: Line and mean opacities for ultracool dwarfs and extrasolar planets. Astrophys. J. Suppl. Ser. **174**, 504–513 (2008). 0706.2374

Freedman, R.S., Lustig-Yaeger, J., Fortney, J.J., Lupu, R.E., Marley, M.S., Lodders, K.: Gaseous mean opacities for giant planet and ultracool dwarf atmospheres over a range of metallicities and temperatures. Astrophys. J. Suppl. Ser. **214**, 25 (2014). 1409.0026

Ginzburg, S., Sari, R.: Tidal heating of young super-Earth atmospheres Mon. Not. R. Astron. Soc. **464**, 3937–3944 (2017). https://arxiv.org/abs/1608.03718

Ginzburg, S., Schlichting, H.E., Sari, R.: Super-Earth atmospheres: self-consistent gas accretion and retention. Astrophys. J. **825**, 29 (2016). 1512.07925

Goldreich, P., Sari, R.: Eccentricity evolution for planets in gaseous disks. Astrophys. J. **585**, 1024–1037 (2003). astro-ph/0202462

Goldreich, P., Lithwick, Y., Sari, R.: Planet formation by coagulation: a focus on Uranus and Neptune. Annu. Rev. Astron. Astrophys. **42**, 549–601 (2004). astro-ph/0405215

Gu, P.G., Lin, D.N.C., Bodenheimer, P.H.: The effect of tidal inflation instability on the mass and dynamical evolution of extrasolar planets with ultrashort periods. Astrophys. J. **588**, 509–534 (2003). astro-ph/0303362

Hayashi, C.: Structure of the solar nebula, growth and decay of magnetic fields and effects of magnetic and turbulent viscosities on the nebula. Prog. Theor. Phys. Suppl. **70**, 35–53 (1981)

Ibgui, L., Burrows, A.: Coupled evolution with tides of the radius and orbit of transiting giant planets: general results. Astrophys. J. **700**, 1921–1932 (2009). 0902.3998

Ibgui, L., Burrows, A., Spiegel, D.S.: Tidal heating models for the radii of the inflated transiting giant planets WASP-4b, WASP-6b, WASP-12b, WASP-15b, and TrES-4. Astrophys. J. **713**, 751–763 (2010). 0910.4394

Ibgui, L., Spiegel, D.S., Burrows, A.: Explorations into the viability of coupled radius-orbit evolutionary models for inflated planets. Astrophys. J. **727**, 75 (2011). 0910.5928

Ikoma, M., Hori, Y.: In Situ accretion of hydrogen-rich atmospheres on short-period super-Earths: implications for the Kepler-11 planets. Astrophys. J. **753**, 66 (2012). 1204.5302

Inamdar, N.K., Schlichting, H.E.: The formation of super-Earths and mini-Neptunes with giant impacts. Mon. Not. R. Astron. Soc. **448**, 1751–1760 (2015). 1412.4440

Inamdar, N.K., Schlichting, H.E.: Stealing the gas: giant impacts and the large diversity in exoplanet densities. Astrophys. J. Lett. **817**, L13 (2016). 1510.02090

Jackson, B., Greenberg, R., Barnes, R.: Tidal heating of extrasolar planets. Astrophys. J. **681**, 1631–1638 (2008). 0803.0026

Jackson, A.P., Davis, T.A., Wheatley, P.J.: The coronal X-ray-age relation and its implications for the evaporation of exoplanets. Mon. Not. R. Astron. Soc. **422**, 2024–2043 (2012). 1111.0031

Jontof-Hutter, D., Rowe, J.F., Lissauer, J.J., Fabrycky, D.C., Ford, E.B.: The mass of the Mars-sized exoplanet Kepler-138 b from transit timing. Nature **522**, 321–323 (2015). 1506.07067

Leconte, J., Chabrier, G., Baraffe, I., Levrard, B.: Is tidal heating sufficient to explain bloated exoplanets? Consistent calculations accounting for finite initial eccentricity. Astron. Astrophys. **516**, A64 (2010). 1004.0463

Lee, E.J., Chiang, E.: To cool is to accrete: analytic scalings for nebular accretion of planetary atmospheres. Astrophys. J. **811**, 41 (2015). 1508.05096

Lee, E.J., Chiang, E.: Breeding super-Earths and birthing super-puffs in transitional disks. Astrophys. J. **817**, 90 (2016). 1510.08855

Lee, E.J., Chiang, E., Ormel, C.W.: Make super-Earths, not Jupiters: accreting nebular gas onto solid cores at 0.1 AU and beyond. Astrophys. J. **797**, 95 (2014). 1409.3578

Lissauer, J.J., Jontof-Hutter, D., Rowe, J.F., Fabrycky, D.C., Lopez, E.D., Agol, E., Marcy, G.W., Deck, K.M., Fischer, D.A., Fortney, J.J., Howell, S.B., Isaacson, H., Jenkins, J.M., Kolbl, R., Sasselov, D., Short, D.R., Welsh, W.F.: All six planets known to orbit Kepler-11 have low densities. Astrophys. J. **770**, 131 (2013). 1303.0227

Liu, X., Burrows, A., Ibgui, L.: Theoretical radii of extrasolar giant planets: the cases of TrES-4, XO-3b, and HAT-P-1b. Astrophys. J. **687**, 1191–1200 (2008). 0805.1733

Liu, S.F., Hori, Y., Lin, D.N.C., Asphaug, E.: Giant impact: an efficient mechanism for the devolatilization of super-Earths. Astrophys. J. **812**, 164 (2015). 1509.05772

Lopez, E.D., Fortney, J.J.: The role of core mass in controlling evaporation: the Kepler radius distribution and the Kepler-36 density dichotomy. Astrophys. J. **776**, 2 (2013). 1305.0269

Lopez, E.D., Fortney, J.J., Miller, N.: How thermal evolution and mass-loss sculpt populations of super-Earths and sub-Neptunes: application to the Kepler-11 system and beyond. Astrophys. J. **761**, 59 (2012). 1205.0010

Lundkvist, M.S., Kjeldsen, H., Albrecht, S., Davies, G.R., Basu, S., Huber, D., Justesen, A.B., Karoff, C., Silva Aguirre, V., Van Eylen, V., Vang, C., Arentoft, T., Barclay, T., Bedding, T.R., Campante, T.L., Chaplin, W.J., Christensen-Dalsgaard, J., Elsworth, Y.P., Gilliland, R.L., Handberg, R., Hekker, S., Kawaler, S.D., Lund, M.N., Metcalfe, T.S., Miglio, A., Rowe, J.F., Stello, D., Tingley, B., White, T.R.: Hot super-Earths stripped by their host stars. Nat. Commun. **7**, 11201 (2016). 1604.05220

Mamajek, E.E.: Initial conditions of planet formation: lifetimes of primordial disks. In: Usuda, T., Tamura, M., Ishii, M. (eds.) American Institute of Physics Conference Series, American Institute of Physics Conference Series, vol. 1158, pp. 3–10 (2009). 0906.5011
Miller, N., Fortney, J.J., Jackson, B.: Inflating and deflating hot Jupiters: coupled tidal and thermal evolution of known transiting planets. Astrophys. J. **702**, 1413–1427 (2009). 0907.1268
Nettelmann, N., Holst, B., Kietzmann, A., French, M., Redmer, R., Blaschke, D.: Ab initio Equation of state data for hydrogen, helium, and water and the internal structure of Jupiter. Astrophys. J. **683**, 1217–1228 (2008). 0712.1019
Owen, J.E., Jackson, A.P.: Planetary evaporation by UV X-ray radiation: basic hydrodynamics. Mon. Not. R. Astron. Soc. **425**, 2931–2947 (2012). 1206.2367
Owen, J.E., Wu, Y.: Kepler planets: a tale of evaporation. Astrophys. J. **775**, 105 (2013). 1303.3899
Owen, J.E., Wu, Y.: Atmospheres of low-mass planets: the "boil-off". Astrophys. J. **817**, 107 (2016). 1506.02049
Piso, A.M.A., Youdin, A.N.: On the minimum core mass for giant planet formation at wide separations. Astrophys. J. **786**, 21 (2014). 1311.0011
Piso, A.M.A., Youdin, A.N., Murray-Clay, R.A.: Minimum core masses for giant planet formation with realistic equations of state and opacities. Astrophys. J. **800**, 82 (2015). 1412.5185
Pollack, J.B., Hubickyj, O., Bodenheimer, P., Lissauer, J.J., Podolak, M., Greenzweig, Y.: Formation of the giant planets by concurrent accretion of solids and gas. Icarus **124**, 62–85 (1996)
Rafikov, R.R.: Atmospheres of protoplanetary cores: critical mass for nucleated instability. Astrophys. J. **648**, 666–682 (2006). astro-ph/0405507
Rafikov, R.R.: Constraint on the giant planet production by core accretion. Astrophys. J. **727**, 86 (2011). 1004.5139
Rogers, L.A., Bodenheimer, P., Lissauer, J.J., Seager, S.: Formation and structure of low-density exo-Neptunes. Astrophys. J. **738**, 59 (2011). 1106.2807
Schlichting, H.E., Warren, P.H., Yin, Q.Z.: The last stages of terrestrial planet formation: dynamical friction and the late veneer. Astrophys. J. **752**, 8 (2012). 1202.6372
Seager, S., Kuchner, M., Hier-Majumder, C.A., Militzer, B.: Mass-radius relationships for solid exoplanets. Astrophys. J. **669**, 1279–1297 (2007). 0707.2895
Teyssandier, J., Ogilvie, G.I.: Growth of eccentric modes in disc-planet interactions. Mon. Not. R. Astron. Soc. **458**, 3221–3247 (2016). 1603.00653
Valencia, D., Pu, M.: Ohmic dissipation in mini-Neptunes. In: AAS/Division for Extreme Solar Systems Abstracts, vol. 3, p. 30105 (2015)
Valencia, D., O'Connell, R.J., Sasselov, D.: Internal structure of massive terrestrial planets. Icarus **181**, 545–554 (2006). astro-ph/0511150
Walker, R.J.: Highly siderophile elements in the Earth, Moon and Mars: update and implications for planetary accretion and differentiation. Chem. Erde-Geochem. **69**, 101–125 (2009)
Weiss, L.M., Marcy, G.W.: The mass-radius relation for 65 exoplanets smaller than 4 earth radii. Astrophys. J. Lett. **783**, L6 (2014). 1312.0936
Williams, J.P., Cieza, L.A.: Protoplanetary disks and their evolution. Annu. Rev. Astron. Astrophys. **49**, 67–117 (2011). 1103.0556
Winn, J.N., Holman, M.J.: Obliquity tides on hot Jupiters. Astrophys. J. Lett. **628**, L159–L162 (2005). astro-ph/0506468
Wolfgang, A., Lopez, E.: How rocky are they? The composition distribution of Kepler's sub-Neptune planet candidates within 0.15 AU. Astrophys. J. **806**, 183 (2015). 1409.2982
Youdin, A.N.: The exoplanet census: a general method applied to Kepler. Astrophys. J. **742**, 38 (2011). 1105.1782